

Cardiovascular, Pulmonary and Renal Pathology

Lack of the Growth Factor Midkine Enhances Survival against Cisplatin-Induced Renal Damage

Hanayo Kawai,^{*,†} Waichi Sato,[†] Yukio Yuzawa,[†]
Tomoki Kosugi,[†] Seiichi Matsuo,[†]
Yoshifumi Takei,^{*} Kenji Kadomatsu,^{*} and
Takashi Muramatsu^{*}

From the Departments of Biochemistry* and Clinical Immunology of Internal Medicine,[†] Nagoya University Graduate School of Medicine, Nagoya, Japan

Although cisplatin acts directly on proximal tubule epithelial cells and causes cell death, little is known regarding the biological significance of its secondary effects, such as inflammation. The growth factor midkine is highly expressed in the proximal tubule and exerts ambivalent activities as to cisplatin nephrotoxicity, ie, anti-apoptotic and chemotactic ones. Here we report that midkine-deficient mice show a significantly higher survival rate than wild-type mice. The levels of blood urea nitrogen and tubular degeneration and apoptosis were higher in wild-type mice despite the anti-apoptotic activity of midkine. We found that recruitment of neutrophils was more enhanced in wild-type mice, this being consistent with the chemotactic activity of midkine. Midkine expression in wild-type mice persisted for 24 hours, and then dramatically decreased. Preadministration of midkine anti-sense oligodeoxyribonucleotide to wild-type mice suppressed midkine expression, and consequently neutrophil infiltration. It is of note that neutrophil infiltration, apoptosis, and elevation of blood urea nitrogen became conspicuous sequentially, namely 1, 2, and 3 days after cisplatin administration, respectively. These findings suggest that early molecular events involving midkine induce inflammatory response and their circuits eventually enhance the death of the proximal tubule epithelial cells. The results indicate the crucial role of inflammation in cisplatin-induced renal damage, and provide a candidate molecular target for its prevention. (*Am J Pathol* 2004, 165:1603–1612)

Cisplatin [*cis*-dichlorodiammine-platinum (II), CDDP] is widely used to treat carcinoma patients. However, its full

clinical utility is significantly limited because of its nephrotoxicity. The main site of CDDP action is in proximal tubule epithelial cells. In proliferating cancer cells, CDDP inhibits DNA and RNA synthesis. In contrast, the effects of CDDP on nonproliferating cells, such as proximal tubule epithelial cells, can be categorized into mainly two primary types.¹ First, CDDP inhibits protein synthesis, probably via nucleolar disruption and disturbance of ribosome assembly.^{2,3} Second, CDDP reduces intracellular glutathione and protein-SH.^{4–7} CDDP exhibits high affinity to SH groups, and thus easily forms protein-S-CDDP adducts. Although this adduct formation may primarily appear as a process of detoxification, it eventually reduces the intracellular contents of glutathione and protein-SH. Because glutathione and protein-SH act as the major cellular oxidant defense system, reduction of their intracellular content leads to membrane lipid peroxidation, DNA damage, and mitochondrial damage. These secondary effects of CDDP may lead to further pathological circuits, such as inflammation, and may make the damage worse. Information regarding the role of the inflammatory mechanism in renal damage induced by CDDP became available very recently.^{8–10}

The heparin-binding growth factor midkine (MK) and pleiotrophin form a family, which is distinct from ones of other heparin-binding growth factors, such as fibroblast growth factors.^{11,12} MK is implicated in nephrogenesis,¹³ and is highly expressed in embryonic as well as adult mouse kidney.^{14–16} In adult mouse kidney, MK is exclusively expressed in the proximal tubule epithelium.¹⁷ It exerts several activities *in vitro*, including anti-apoptotic and chemotactic ones.^{18–22} Using MK-deficient (*Mdk*^{-/-}) mice, a pivotal role of MK in the recruitment of inflammatory cells was revealed in two disease models.^{17,21} In an artery restenosis model, *Mdk*^{-/-} mice exhibit significantly less neointima formation as compared with wild-type (*Mdk*^{+/+}) mice.²¹ The neointima is

Supported by grants-in-aid from the Ministry of Education, Science, Sports, and Culture of Japan (15390103 to T.M.; 14580647 to K.K.).

Accepted for publication July 14, 2004.

Address reprint requests to Professor Takashi Muramatsu: Department of Biochemistry, Nagoya University Graduate School of Medicine, 65 Tsurumai-cho, Showa-ku, Nagoya 466-8550, Japan. E-mail: tmurama@med.nagoya-u.ac.jp.

the basic lesion of blood vessel restenosis and atherosclerosis, and its formation is induced by recruited inflammatory cells, such as neutrophils and macrophages. In a reperfusion renal injury model, *Mdk*^{-/-} mice also exhibit less damage.¹⁷ In this model, the inflammatory cells are again key players. Consistent with the *in vitro* chemotactic activity of MK,^{20,21} inflammatory cell recruitment is significantly suppressed in *Mdk*^{-/-} mice in both models.^{17,21}

Another important activity of MK is an anti-apoptotic one.^{18,19} MK inhibits the apoptosis of neuronal cells induced by serum starvation.¹⁹ MK prevents degeneration of photoreceptor cells induced by constant light exposure of the eye.²³ MK also exerts an anti-apoptotic effect in brain infarction.²⁴ MK induces Bcl-2 in G401 Wilms' tumor cells, to which, at least in part, anti-apoptotic activity of MK may be attributed.¹⁸ Thus, MK has ambivalent activities with respect to CDDP-induced renal damage; an anti-apoptotic one that makes mice resistant to CDDP, and a chemotactic one that makes mice sensitive to CDDP. Therefore, we expected that MK-deficient mice would provide a good model for dissecting the mechanistic sequence of CDDP-induced renal damage, and for evaluating the biological significance of inflammation and apoptosis.

Materials and Methods

Chemicals and Other Reagents

CDDP was obtained from Bristol-Myers (Tokyo, Japan). Kits for measuring BUN (blood urea nitrogen) were purchased from Wako (Osaka, Japan). Medium and reagents for cell culture were purchased from Sigma Chemical Co. (St. Louis, MO). Fetal bovine serum, penicillin/streptomycin, and trypsin/ethylenediaminetetraacetic acid solution were from Life Technologies, Inc. (Gaithersburg, MD). OCT compound was from Tissue Tec, Miles Laboratories (Elkhart, IN).

Primary Antibodies and Secondary Reagents

Rabbit anti-MK antibody was prepared as described previously.²⁵ Monoclonal anti- β -actin antibody was obtained from Sigma-Aldrich (St. Louis, MO). Monoclonal rat anti-mouse neutrophil marker 7/4 antibody was purchased from Serotec Ltd. (Oxford, UK). Fluorescein isothiocyanate-conjugated rabbit anti-rat IgG was from ICN Pharmaceuticals, Inc. (Aurora, OH). Rat antibody against the mouse leukocyte common antigen CD45 was from PharMingen (San Diego, CA). Rat antibody against the mouse macrophage F4/80 antigen was purchased from Serotec Ltd. Fluorescein isothiocyanate anti-mouse CD4 (clone GK1.5) and fluorescein isothiocyanate anti-mouse CD8 (clone 53-6.7) were obtained from eBioscience (San Diego, CA). Anti-mouse Bcl-2 antibody was from Upstate Biotechnology (Lake Placid, NY). Rabbit anti-Bcl_{xL} antibody, rabbit anti-mouse BAX antibody, rabbit anti-Bak antibody, rabbit anti-Bid antibody, and rabbit anti-caspase3 antibody were purchased from BD Bio-

sciences PharMingen, San Diego, CA. Peroxidase-conjugated rabbit IgG and mouse IgG were from Jackson ImmunoResearch Laboratories, Inc. (West Grove, PA).

Animal Treatment and CDDP Administration

Experiments were performed on 8- to 12-week-old male 129SV wild-type (*Mdk*^{+/+}) mice or MK-deficient (*Mdk*^{-/-}) mice weighing 25 to 30 g. *Mdk*^{-/-} mice were generated as described previously.²⁶ After backcrossing of *Mdk*^{+/-} mice for 12 generations to *Mdk*^{+/+} mice, *Mdk*^{+/-} mice were mated with each other to generate the *Mdk*^{+/+} and *Mdk*^{-/-} mice that were used in this study. Mice were housed under controlled environmental conditions, and maintained with standard food and water. Mice were randomly divided into two groups; one was given a single intraperitoneal injection of saline and the other group of CDDP at the indicated dose (10 to 14 mg/kg of body weight). The mice were sacrificed at 1, 2, 3, and 5 days after injection. Blood samples were collected from the suborbital sinus on the day of sacrifice. Tissue from the kidneys was processed for histology and for protein and mRNA extraction. For measuring CDDP concentration in urine, mice were injected intraperitoneally with 12 mg/kg of *cis*-platin and housed individually in metabolic cages for 24 hours, and urine was collected in ice-cooled containers for 24 hours after dosing. CDDP concentrations were measured by NAC Co., Ltd. (Tokyo, Japan). The experiments described above were all conducted according to the Animal Experimentation Guide of Nagoya University Graduate School of Medicine.

Survival Course

The survival course of mice given CDDP at 14 mg/kg was examined. After CDDP injection, mice were monitored daily for 7 days. The results were statistically assessed.

Morphology Assessment

The removed kidneys were fixed in 4% paraformaldehyde, embedded in paraffin, and then cut into 2- μ m sections. Also, tissues were embedded in OCT and frozen in liquid nitrogen. Four- μ m sections were cut with a cryostat and placed on slides coated with 3-aminopropyltriethoxysilane. The tissues were stained with periodic acid-Schiff's reagent. The degree of morphological changes was determined by light microscopy, and tubulointerstitial damage was scored on a semiquantitative scale as described previously.²⁷ Briefly, the extents of tubular cast formation, tubular dilatation, and tubular degeneration (vascular change, loss of brush border, detachment of tubular epithelial cells, and condensation of tubular nuclei) were scored according to the following criteria by two observers in a blind manner: 0, normal; 1, less than 30% of the pertinent area; 2, 30 to 70%; 3, more than 70%.

Apoptosis Detection and Quantification

The detection of *in situ* apoptosis using the terminal dUTP nick-end labeling (TUNEL) method was performed following the manufacturer's technique (Takara Biomedical, Osaka, Japan). Eighteen 10 × 20 fields were examined to count apoptotic cells.

Infiltrating Cell Count

Cryosections were immunohistochemically stained with the antibodies for neutrophils, macrophages, and T cells, respectively. Eighteen 10 × 20 fields were examined to count infiltrating cells.

Primary Culture of Proximal Tubular Epithelial Cells

Proximal tubular epithelial cells were isolated from the kidneys of adult *Mdk*^{+/+} or *Mdk*^{-/-} mice, and then cultured in K1 medium (224.25 ml of Ham's F12, 226.25 ml of Dulbecco's modified Eagle's medium, and 12.5 ml of HEPES) containing 10% fetal bovine serum and hormones, as described previously.²⁸ They were determined to be of proximal tubular origin by immunofluorescent histochemistry: cells were stained positively for cytokeratin (Enzo Diagnostics, Inc., Farmingdale, NY), vimentin (ICN Biomedicals Inc.), and alkaline phosphatase, but negatively for CD31 (BD Biosciences Pharmingen) and α -smooth muscle actin.

At the confluent state, cells were exposed to 0 to 50 μ mol/L CDDP in K1 medium for 24 hours or to 40 μ mol/L CDDP for 0, 3, 6, 12, 18, or 24 hours. Cells were then lysed in ice-cold RIPA buffer (comprising 50 mmol/L Tris-HCl, 150 mmol/L NaCl, 1% Nonidet P, 1% deoxycholic acid, and 0.05% sodium dodecyl sulfate) with 0.25 mmol/L phenylmethyl sulfonyl fluoride, kept on ice for 60 minutes, and then centrifuged at 15,000 × *g* for 10 minutes at 4°C. The supernatants were then subjected to sodium dodecyl sulfate-polyacrylamide gel electrophoresis and Western blotting.

Primary Culture of Mouse Embryonic Fibroblasts (MEFs)

MEFs were derived from 15-day-old embryos according to standard protocols.²⁹ MEFs were cultured in a 60-mm-diameter culture dish in Dulbecco's modified Eagle's medium containing 10% fetal bovine serum. For 3-(4,5-dimethyl-2-thiazolyl)-2,5-diphenyl-2H-tetrazolium bromide (MTT) assay, 1.0 × 10⁴ cells/well were seeded in 96-well plates and allowed to adhere overnight. Serial dilutions of CDDP were added to wells at concentrations from 1 to 50 μ mol/L, and cells were exposed to CDDP for an additional 72 hours. MTT assay was performed according to the manufacturer's instructions (Cell Counting kit, Wako).

Western Blotting

Mouse kidney tissues were snap-frozen in liquid nitrogen for protein isolation. Proteins were extracted by homogenization of the tissues in ice-cold RIPA buffer (comprising 50 mmol/L Tris-HCl, 150 mmol/L NaCl, 1% Nonidet P, 1% deoxycholic acid, and 0.05% sodium dodecyl sulfate) with 0.25 mol/L phenylmethyl sulfonyl fluoride, and centrifugation at 15,000 × *g* for 60 minutes at 4°C. The supernatants were then subjected to sodium dodecyl sulfate-polyacrylamide gel electrophoresis and Western blotting. Proteins were visualized using the enhanced chemiluminescence detection system (Amersham Pharmacia, Amersham Biosciences, Piscataway, NJ).

Northern Blotting

Mouse kidney tissues were snap-frozen in liquid nitrogen for total mRNA isolation as described previously.³⁰ To standardize the Northern blots, we used a probe for a housekeeping protein, GAPDH, as the internal control. Chemokine expression including MCP-1, MIP-2, RANTES, and keratinocyte-derived chemokine (KC) were assessed.

KC Protein Enzyme-Linked Immunosorbent Assay (ELISA)

After protein extraction from mouse kidney tissue, KC levels were measured using an ELISA kit (IBL Co., Ltd., Gunma, Japan) according to the manufacturer's instructions. Results were normalized to total protein concentration.

RNase Protection Assay

Total mRNA was subjected to RNase protection assay using the multiprobe ribonuclease protection assay system (mouse CK-5c probe set; BD Biosciences Pharmingen) according to the manufacturer's instructions. Multiprobe includes cDNAs for nine proteins, lymphotactin, RANTES, MIP-1 α , MIP-1 β , MIP-2, IP-10, MCP-1, TCA-3, and eotaxin, and two cDNAs for housekeeping proteins, L32 and GAPDH. The bands were quantified with a PhosphorImager using ImageQuant software (Amersham Biosciences K.K., Tokyo, Japan), and the chemokine mRNA levels were normalized as to the L32 mRNA levels.

In Vivo Administration of Anti-Sense Oligodeoxyribonucleotide (ODN) Targeted to MK

Mouse MK anti-sense (AS)- and reverse (R)-ODNs were prepared as described previously.³¹ The sequences were as follows. AS, 5'-AGGGCGAGAAGGAAGAAG-3'; R, 5'-GAAGAAGGAAGAGCGGGA-3'. AS or R ODN (1 mg/kg of body weight) were dissolved in 150 μ l of saline and injected intravenously via tail vein before administration of *cis*-platin. For evaluation of AS effect on CDDP

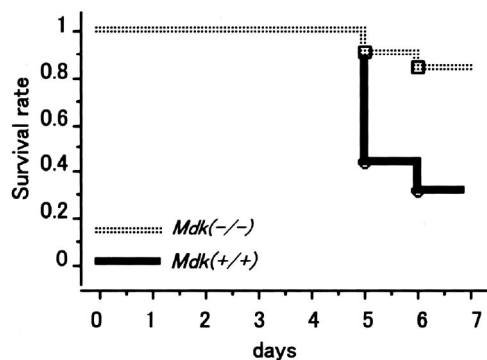


Figure 1. Survival course of mice injected with 14 mg of CDDP/kg. At day 7, the survival rate of *Mdk*^{+/+} was 30% and that of *Mdk*^{-/-} was ~90%. The **solid line** indicates *Mdk*^{+/+} and the **dotted line** indicates *Mdk*^{-/-} mice. *n* = 34; *P* < 0.01 (log rank test).

nephrotoxicity, we counted the infiltrating neutrophils on day 1.

Statistical Analysis

All data are expressed as means ± SE. Statistical analysis was performed with unpaired, two-tailed Student's *t*-test for single comparisons or analysis of variance for multiple comparisons. In the survival course experiment, statistical significance was assessed with log rank. A *P* value < 0.05 was taken to indicate a significant difference.

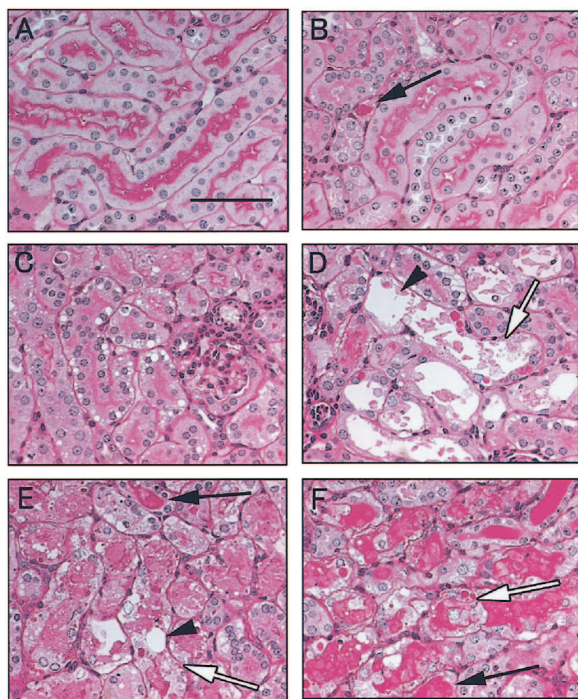


Figure 2. Histological evaluation of *Mdk*^{+/+} mice at day 5 with several doses of CDDP by periodic acid-Schiff staining. Each picture depicts tubulointerstitial damage in *Mdk*^{+/+} mice on day 5 after injection of CDDP. **A:** Normal control; **B:** 10 mg/kg CDDP; **C:** 11 mg/kg CDDP; **D:** 12 mg/kg CDDP; **E:** 13 mg/kg CDDP; **F:** 14 mg/kg CDDP. **Arrow**, cast formation; **arrowhead**, tubular dilation; **open arrow**, tubular degeneration. Scale bar, 50 μm.

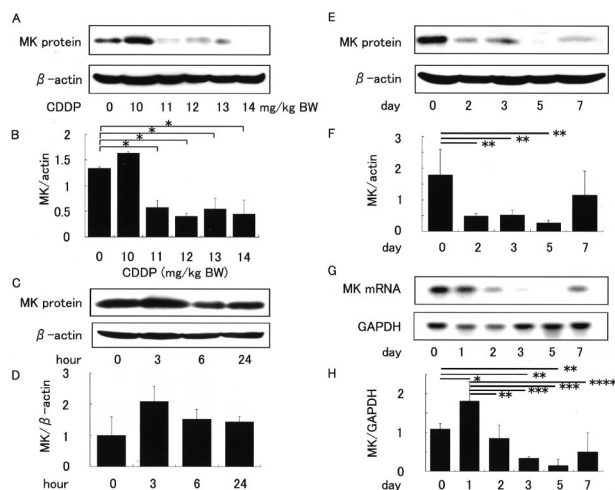


Figure 3. MK expression after injection of CDDP into *Mdk*^{+/+} mice. **A:** MK protein levels in kidneys from CDDP-injected *Mdk*^{+/+} mice examined by Western blotting. The CDDP dose ranged from 10 mg/kg to 14 mg/kg. The kidneys were taken on day 5 when the most severe damage appeared. **B:** Intensity of MK bands in **A** were normalized as to β-actin. Data are means ± SE (*n* = 3). *, *P* < 0.001 versus control. Mice were injected with CDDP at 12 mg/kg in the experiments from **C** to **H**. **C:** Time course of MK protein expression during the first 24 hours. **D:** Normalized intensity of MK bands in **C**. Data are means ± SE (*n* = 6). **E:** Time course of MK protein expression by day 7. **F:** Normalized intensity of MK bands in **E**. Data are means ± SE (*n* = 6). **, *P* < 0.005 versus day 0. **G:** Time course of MK mRNA expression. **H:** Normalized intensity of MK mRNA bands in **G**. Data are means ± SE (*n* = 6). *, *P* < 0.05 versus day 0; **, *P* < 0.005 versus day 0 or 1; ***, *P* < 0.0001 versus day 1; ****, *P* < 0.0005 versus day 1.

Results

Mdk^{-/-} Mice Exhibit Less Mortality on CDDP Treatment

We examined the survival courses of *Mdk*^{+/+} and *Mdk*^{-/-} mice by injecting 14 mg of CDDP/kg of body weight. Almost 90% of the *Mdk*^{-/-} mice exhibited 7-day survival. In contrast, only 30% of the *Mdk*^{+/+} mice survived (Figure 1). There was a statistically significant difference between the two genotypes (*P* < 0.01).

CDDP Induces Less Renal Damage in *Mdk*^{-/-} Mice

Because most mice injected with 14 mg/kg of CDDP died of acute renal failure by day 7 (Figure 1), we intended to determine the appropriate dose for monitoring changes in the kidney. The histology of *Mdk*^{+/+} mice 5 days after CDDP injection is shown in Figure 2. Renal damage was manifested as cast formation, tubular dilation, and tubular degeneration. Although there was negligible damage with 10 mg/kg (Figure 2B), damage became more severe with increasing dose of CDDP more than 11 mg (Figure 2; C to F). The MK protein expression profile also showed an apparent threshold. MK protein expression did not show any changes at day 5 with 10 mg/kg as compared with an untreated control, but was dramatically suppressed with more than 11 mg/kg (Figure 3, A and B). In contrast to histological changes that became progressively worse with increasing doses, MK protein expression was sup-

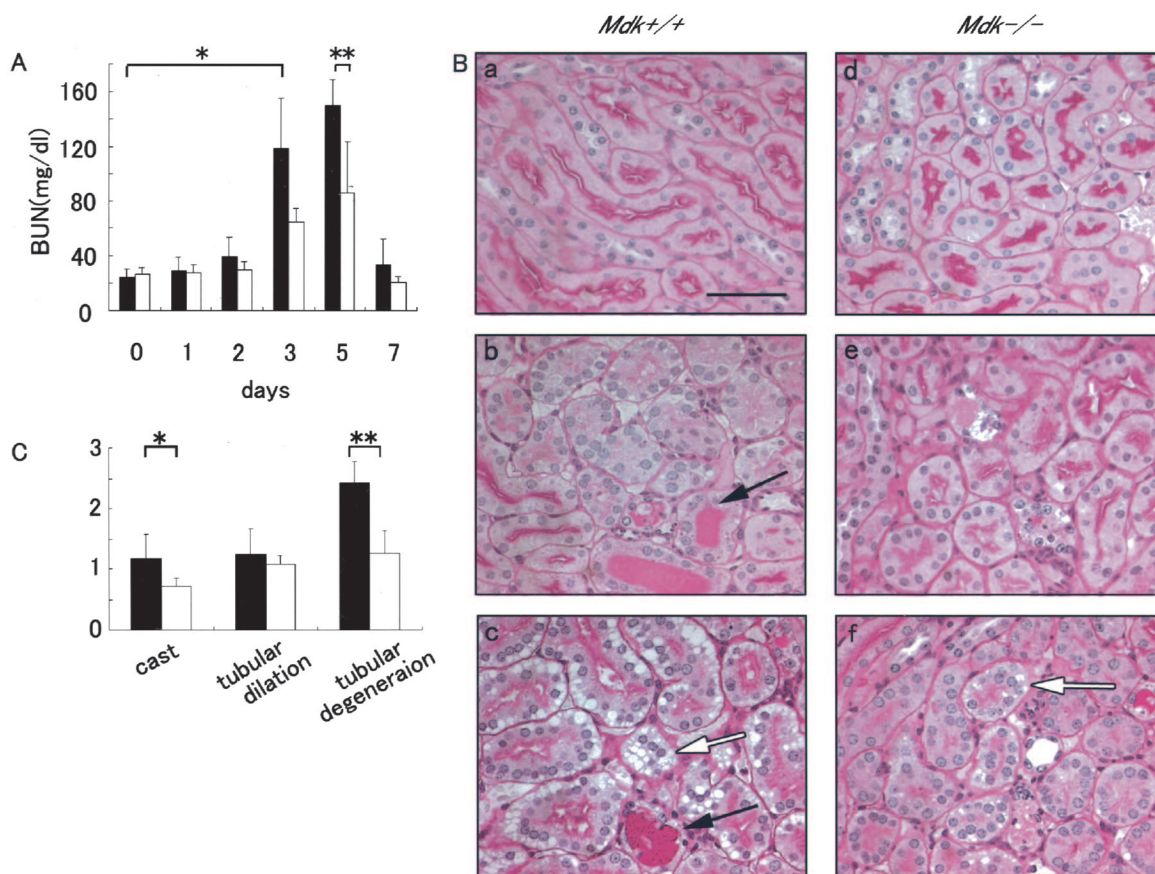


Figure 4. Histological evaluation and BUN of *Mdk*^{+/+} and *Mdk*^{-/-} mice injected with 12 mg of CDDP/kg. **A:** BUN (mean \pm SE) is shown ($n = 6$). ■, *Mdk*^{+/+} mice; □, *Mdk*^{-/-} mice. *, $P < 0.05$ versus wild normal control; **, $P < 0.001$. **B:** Tubulointerstitial damage on days 0, 3, and 5 (periodic acid-Schiff staining) is shown. **a**, *Mdk*^{+/+} day 0; **b**, *Mdk*^{+/+} day 3; **c**, *Mdk*^{+/+} day 5; **d**, *Mdk*^{-/-} day 0; **e**, *Mdk*^{-/-} day 3; **f**, *Mdk*^{-/-} day 5. **Arrow**, cast formation; **open arrow**, tubular degeneration. **C:** Semiquantitative analysis of tubulointerstitial damage. The degrees of damage including cast formation, tubular dilation, and tubular degeneration were scored according to the method described in Materials and Methods. These are the results on day 5. More severe damage is indicated by higher values. Data are means \pm SE ($n = 6$). *, $P < 0.05$; **, $P < 0.005$. Scale bar, 50 μ m (**a-e**).

pressed to a similar extent if the dose was more than 11 mg/kg (Figure 3, A and B). This suggests that a lower dose (eg, 11 or 12 mg/kg) is sufficient to determine the effect of MK protein expression (eg, *Mdk*^{+/+} versus *Mdk*^{-/-}), and has the advantage of reducing the background pathological changes induced by high-dose CDDP. In addition, a lower dose, unlike 14 mg/kg, was not lethal (data not shown), so we were able to monitor the kidney without postmortem changes. Therefore, we chose the dose of 12 mg/kg for further experiments.

We examined the time course of MK protein expression in kidneys from *Mdk*^{+/+} mice. MK protein expression tended to be increased by 24 hours after CDDP administration although no statistical difference was obtained, and then dramatically decreased, reaching the lowest level on day 5 (Figure 3; C to F). MK mRNA expression showed a profile similar to that of protein, but exhibited a statistical difference at day 1 as compared with day 0 (Figure 3, G and H), suggesting that posttranscriptional regulation is also involved in MK protein expression.

Renal function and tissue morphology were then evaluated by means of BUN and histology, respectively. In *Mdk*^{+/+} mice, BUN elevation became prominent at day 3 as compared with at day 0 (Figure 4A). *Mdk*^{+/+} mice showed a worse phenotype than *Mdk*^{-/-} mice in terms

of BUN and histology (Figure 4). There were significant differences between these genotypes on day 5 in BUN, tubular degeneration, and cast formation (Figure 4, A and C). However, a critical event was expected to take place earlier, because, at a later stage (later than day 2), MK expression was strongly suppressed in *Mdk*^{+/+} mice (Figure 3; E to H), and was negative in *Mdk*^{-/-} mice.

Apoptosis Was Less in *Mdk*^{-/-} Mice

To elucidate the mechanisms underlying the different sensitivities of *Mdk*^{+/+} and *Mdk*^{-/-} mice to CDDP, we next examined apoptosis. As compared with on day 0, apoptotic cells became conspicuous on day 2 in both *Mdk*^{+/+} and *Mdk*^{-/-} mice ($P < 0.05$) (Figure 5B). The apoptotic cell count was significantly less in *Mdk*^{-/-} mice on day 5 ($P < 0.001$) (Figure 5, A and B). This result was contrary to that expected from the anti-apoptotic activity of MK.^{18,19} As shown in Figure 5C, most of the apoptotic cells were not positive with the anti-CD45 antibody, which is a marker of inflammatory cells, indicating that apoptotic cells were probably proximal tubular cells but not inflammatory cells.

Expression of Bcl-2 family members including Bcl-x_L, BAX, Bid, and Bak in the kidney did not differ between

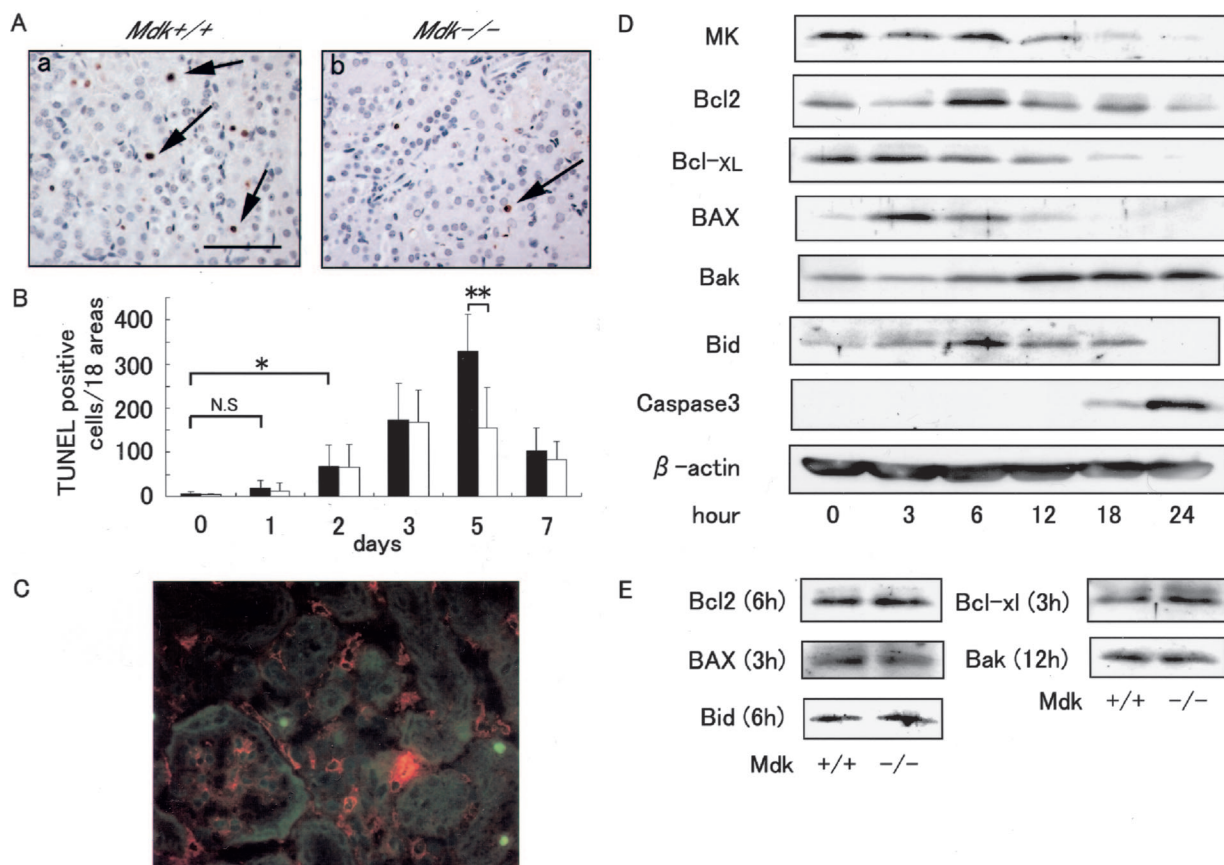


Figure 5. *In situ* apoptosis detection in CDDP-injected *Mdk*^{+/+} and *Mdk*^{-/-} mice kidneys. **A:** Paraffin-embedded kidney sections were subjected to *in situ* apoptosis detection with the TUNEL method. These are representatives on day 5. **Arrows** indicate some of the positively stained cells. **a,** *Mdk*^{+/+}; **b,** *Mdk*^{-/-}. **B:** The numbers of TUNEL-positive cells on days 0, 1, 2, 3, 5, and 7 were determined. They were scored by examining 18 regions under a microscope at ×400 magnification. Data are means ± SE (n = 6). ■, *Mdk*^{+/+} mice; □, *Mdk*^{-/-} mice; N.S., not significant; *, P < 0.001 versus wild normal control; **, P < 0.005. **C:** Double staining with CD45 (red) and TUNEL (green). The section was for an *Mdk*^{+/+} mouse on day 5. **D:** Time course of Bcl-2 family protein expression in CDDP-stimulated *Mdk*^{+/+} tubular epithelial cells. The results of Western blotting are shown. **E:** Bcl-2 family expression in *Mdk*^{+/+} and *Mdk*^{-/-} tubular epithelial cells. Scale bar, 50 μm.

Mdk^{+/+} and *Mdk*^{-/-} mice (data not shown). We could detect a trace level of Bcl-2 expression in the whole kidney. Tubular epithelial cells were thus prepared from *Mdk*^{+/+} and *Mdk*^{-/-} mice. Tubular epithelial cells expressed Bcl-2 at 3 hours after CDDP stimulation, with a peak at 6 hours (Figure 5D). However, there was no significant difference between *Mdk*^{+/+} and *Mdk*^{-/-} mice (Figure 5E). Bcl-xL decreased gradually with time after CDDP treatment (Figure 5D). BAX and Bid exhibited peaks at 3 to 6 hours, and that of Bak was at 12 hours after CDDP treatment (Figure 5D). Also there were no differences between *Mdk*^{+/+} and *Mdk*^{-/-} mice in these expressions (Figure 5E). Thus, we could not find any relation between the anti-apoptotic effect of MK and Bcl-2 family proteins in primarily cultured tubular epithelial cells.

No Differences in Susceptibility to CDDP and Delivery of CDDP in *Mdk*^{+/+} and *Mdk*^{-/-} Mice

The differences of CDDP nephrotoxicity between *Mdk*^{+/+} and *Mdk*^{-/-} mice might be because of a dif-

ference in general susceptibility to CDDP or delivery of CDDP to tubule cells. To address this question, we examined cell survival of MEFs derived from *Mdk*^{+/+} and *Mdk*^{-/-} mice against several doses of CDDP and measured the CDDP in urine. There were no differences in susceptibility at any doses (1 to 50 μmol/L) of CDDP (Figure 6A). With regards to the delivery of CDDP to tubule cells, we found no differences of CDDP in urine between *Mdk*^{+/+} and *Mdk*^{-/-} mice (Figure 6B).

Leukocyte Infiltration into the Tubulointerstitium Was Less in *Mdk*^{-/-} Mice

Another important activity of MK is a chemotactic one. Therefore, we determined the number of neutrophils that invaded the tubulointerstitium. Although detectable renal damage, as assessed by means of histology and BUN, appeared on day 3 (Figure 4), and apoptosis became prominent on day 2 (Figure 5), neutrophil infiltration was recognized on day 1 in *Mdk*^{+/+} mice (P < 0.005 versus day 0) (Figure 7, A and B). In *Mdk*^{+/+} mice, neutrophil infiltration reached the maximum level on day 5, and then decreased. In contrast, it became apparent on day 2

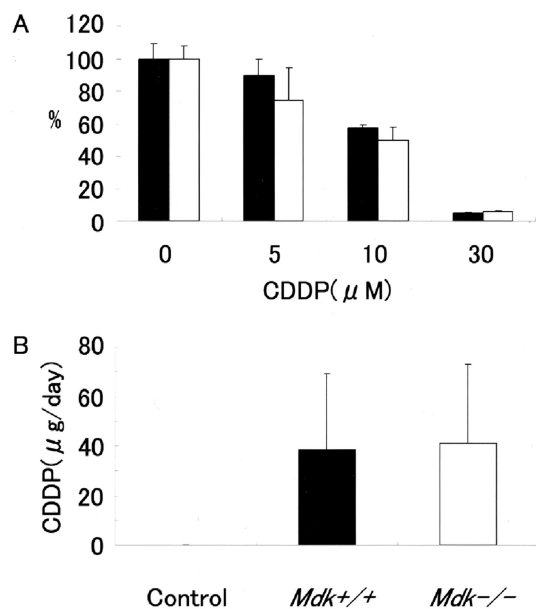


Figure 6. Cell survival and susceptibility against CDDP. **A:** Cell survival, expressed as percentage of the control (% means \pm SE) of MEFs after 72 hours of incubation. MEFs were continuously exposed to CDDP with indicated doses for 72 hours. Survival was determined by using a cell counting kit. $n = 3$. ■, MEFs from *Mdk*^{+/+} mice; □, *Mdk*^{-/-} mice. There were no significant differences between *Mdk*^{+/+} and *Mdk*^{-/-} mice. **B:** CDDP urinary excretion. After CDDP injection, urine was collected for the next 24 hours. CDDP concentration was determined as described under Materials and Methods. Data are means \pm SE ($n = 4$). There were no significant differences in urinary CDDP concentration between *Mdk*^{+/+} and *Mdk*^{-/-} mice.

($P < 0.005$ versus day 0), reaching the maximum level on day 3 in *Mdk*^{-/-} mice. Thus, *Mdk*^{+/+} mice showed rapid induction and prolonged persistence of neutrophil infiltration, whereas *Mdk*^{-/-} mice exhibited slow induction and rapid fading. Consequently, the number of infiltrating neutrophils was significantly lower in *Mdk*^{-/-} as compared with in *Mdk*^{+/+} mice on days 1 and 5 (Figure 7B).

We also investigated infiltration of other important inflammatory cells, ie, macrophages and T cells. We found apparent infiltration (statistically different from day 0) of macrophages, CD4-positive T cells and CD8-positive T cells on days 2, 3, and 2, respectively, in *Mdk*^{+/+} mice (Figure 7C, macrophage; Figure 7Da, CD4-positive T cells; Figure 7Db, CD8-positive T cells). We also found statistical differences between *Mdk*^{+/+} and *Mdk*^{-/-} mice on days 5, 3, and 7, respectively. The results also indicated that neutrophil infiltration was the earliest event in inflammatory cell infiltration (Figure 7B).

MK is known to induce chemokines in the ischemic reperfusion injury model of the kidney.¹⁷ We thus investigated whether or not chemokines were induced in this CDDP-induced renal damage model. It is well known that KC acts as chemoattractant for neutrophils. ELISA assay showed that KC protein was slowly induced in damaged kidney, whereas we could not find any differences between *Mdk*^{+/+} and *Mdk*^{-/-} mice (Figure 7Ea). KC mRNA expression as revealed by Northern blotting showed results similar to those of protein (Figure 7Eb). The expression of chemokines, such as MCP-1 and MIP-2, was not detectable on Northern blot analysis in the

CDDP model (data not shown), which was in contrast to in the case of the ischemic reperfusion injury model.¹⁷ To examine induction of other chemokines, we performed the RNase protection assay. Lymphotactin and MIP-2 were induced from day 2 and reached peaks on day 3 (Figure 7E, c and d). However, there were no significant differences in these expression between *Mdk*^{-/-} and *Mdk*^{+/+} mice. The expression of other chemokines, including RANTES, MIP-1 α , MIP-1 β , IP-10, MCP-1, TCA-3, and eotaxin, was also low and was not different between the two genotypes (data not shown). These results suggest that, even though low expression of chemokines would contribute to neutrophil infiltration, MK plays a direct critical role in the inflammation in the CDDP model.

MK AS ODN Ameliorates Neutrophil Infiltration

To further prove the importance of MK in this model, we used mouse MK AS ODN that had been established in our laboratory.³¹ MK protein expression was most suppressed when AS ODN was injected via tail vein 16 to 24 hours before sacrifice (Figure 8, A and B). In contrast to AS ODN, reverse control (R) did not suppress MK protein expression 24 hours after ODN administration (Figure 8C). We speculated that MK was involved in early event of CDDP nephrotoxicity, especially in neutrophil recruitment. Thus, we decided to inject AS ODN before CDDP administration. MK AS ODN injected 24 hours before CDDP administration significantly suppressed the numbers of infiltrating neutrophils on day 1 (24 hours after CDDP administration), as compared with MK R ODN (Figure 8E).

Discussion

The ambivalent activities of MK, ie, anti-apoptotic and chemotactic ones, provide an intriguing model for CDDP-induced renal injury. In the present study, we used wild-type (*Mdk*^{+/+}) and MK-deficient (*Mdk*^{-/-}) mice to investigate the mechanism underlying the pathogenesis. Despite strong suppression of MK expression at a later stage (ie, later than day 2), *Mdk*^{+/+} mice manifested the worse phenotypes. As the basis of the above phenomena, we found that neutrophil infiltration was significantly different between the two genotypes, and MK expression persisted by day 1 when neutrophil infiltration into the tubulointerstitium had become prominent. Unlike the ischemic reperfusion injury model, in which chemokines are strongly induced, only low induction of chemokines was detected in the CDDP model, and there was no difference between the two genotypes. Therefore, it is most likely that the existence of MK protein at early phase in the milieu of CDDP-damaged tissue is needed for the secondary effect of CDDP, ie, inflammation, especially neutrophil infiltration. This idea was supported by the finding that MK knockdown by MK AS ODN led to suppression of neutrophil infiltration (Figure 8). We speculate that molecular circuits involving MK participate in early phase to induce inflammation. Such molecular circuits may initiate chain reactions, which make the inflammation

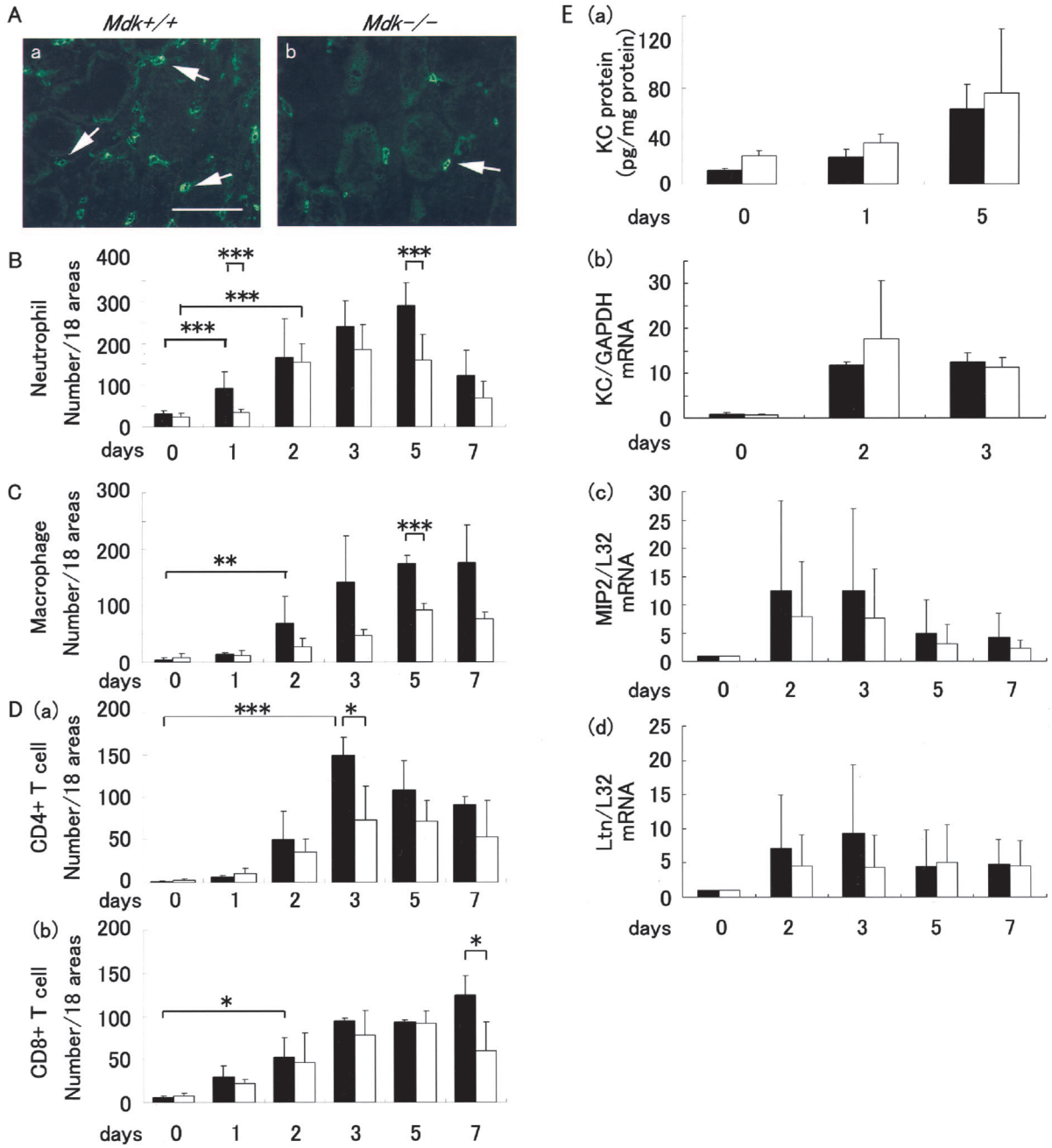


Figure 7. Quantitative analysis of infiltrating cells and chemokines. **A:** **a**, Neutrophil infiltration in *Mdk*^{+/+}; **b**, *Mdk*^{-/-}. These are representatives of day 5. **Arrows** indicate some positive cells. **B:** The numbers of infiltrating neutrophils on the indicated days were determined. They were scored by examining 18 regions under a microscope at $\times 200$ magnification. Data are means \pm SE ($n = 6$ except day 1; $n = 10$ for day 1). \blacksquare , *Mdk*^{+/+} mice; \square , *Mdk*^{-/-} mice. *******, $P < 0.005$. **C:** The numbers of infiltrating macrophages. ******, $P < 0.01$; *******, $P < 0.005$. **D:** **a**, The numbers of infiltrating CD4-positive T cells. *****, $P < 0.05$; *******, $P < 0.005$. **b**, The numbers of infiltrating CD8-positive T cells. *****, $P < 0.05$. **E:** Chemokine expression. **a**, KC protein expression examined by ELISA. Data were normalized to total protein concentration. Data are means \pm SE ($n = 3$). **b**, KC mRNA expression examined by Northern blotting. Data were normalized to GAPDH mRNA. Data are means \pm SE ($n = 3$). **c**, MIP-2 expression examined by RNase protection assay. The relative ratios of MIP-2/L32 are shown. **d**, Lymphotactin expression examined by RNase protection assay. The relative ratios of Ltn/L32 are shown. Scale bar, 50 μ m. Original magnifications, $\times 400$.

worse and consequently enhance the death of the proximal tubule epithelial cells. This idea explains why we observed significant differences in apoptosis, BUN, and histological damages in late phase, on day 5, between *Mdk*^{+/+} and *Mdk*^{-/-} mice in this study.

Although it is known that MK has chemotactic activity to neutrophils and macrophages,^{20,21} there are no reports for T cells. No matter how MK exhibits effects on

chemotaxis of macrophages and T cells, differences of infiltration of these cells between *Mdk*^{+/+} and *Mdk*^{-/-} mice became apparent in later time points, when MK expression is lower than the normal level in *Mdk*^{+/+} mice. Therefore, the above-mentioned chain reactions initiated by neutrophil infiltration in the early stage may eventually influence the recruitment of other leukocytes in later stages. However, we do not exclude the possibility

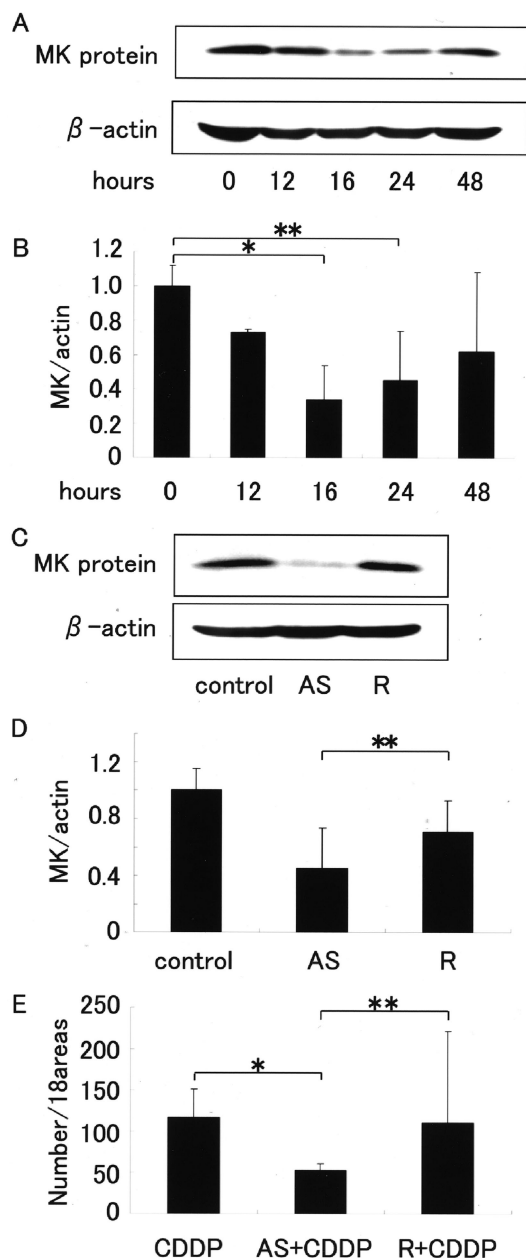


Figure 8. MK AS ODN treatment. **A:** MK protein levels in kidneys from AS-injected *Mdk*^{+/+} mice examined by Western blotting. Mice were sacrificed at the indicated hours after MK AS ODN administration via tail vein. **B:** Intensity of MK bands in **A** was normalized as to β -actin. Data are means \pm SE ($n = 3$). *, $P < 0.01$; **, $P < 0.05$ versus control. **C:** MK protein levels in kidneys from MK anti-sense (AS) or reverse (R) ODN-injected *Mdk*^{+/+} mice at 24 hours after ODN administration. **D:** Intensity of MK bands in **C** was normalized as to β -actin. Data are means \pm SE ($n = 6$). **, $P < 0.05$ versus AS-treated mice. There was no significant difference in MK expression between untreated and MK R ODN-injected mice. **E:** The numbers of infiltrating neutrophils. Mice had been administered with MK AS ODN 24 hours before CDDP injection, and were sacrificed on day 1 (24 hours after CDDP). They were scored by examining 18 regions under a microscope at $\times 200$ magnification. Data are means \pm SE ($n = 6$). ***, $P < 0.005$ versus wild control-injected only CDDP; **, $P < 0.05$ AS versus R.

that MK expressed in a minimal amount in later stages might collaborate with inflammatory reactions initiated by early phase neutrophil infiltration, and contribute to the infiltration of macrophages and T cells in later stages,

which could influence renal damages as estimated by apoptosis, BUN, and histological changes.

MK exhibited anti-apoptotic activity toward Wilms' tumor cells, which were used as a model of tubular epithelial cells.¹⁸ However, these experiments were performed *in vitro*. We consider that, *in vivo*, the anti-apoptotic activity of endogenous MK was overwhelmed by enhanced leukocyte migration caused by MK. Concerning the *in vitro* anti-apoptotic activity of MK toward neuronal cells,¹⁹ we confirmed the activity *in vivo*: exogenously supplied MK inhibits retinal cell degeneration caused by exposure to constant light²³ and delayed death of hippocampal neurons.²⁴ With a large dose of exogenously supplied MK, the anti-apoptotic activity might become more conspicuous. Therefore, we cannot exclude the possibility that MK prevents the damage of tubular epithelial cells, when it is supplied in a large quantity by means of a suitable method.

One of the direct actions of CDDP is the formation of CDDP-glutathione conjugate,^{32,33} which is subsequently metabolized to CDDP-cysteinyglycine conjugates via γ -glutamyl transpeptidase in the proximal tubules. The conjugates may be further cleaved to cysteine-conjugates by aminopeptidase, which is also on the surface of the cells. CDDP-glutathione conjugates, CDDP-cysteinyglycine conjugates, and CDDP-cysteine conjugates are more toxic to proximal tubule cells than CDDP.³⁴ Indeed, γ -glutamyl transpeptidase-deficient mice exhibit resistance to the nephrotoxic effects of CDDP.³⁵ In many studies on CDDP nephrotoxicity, much attention was focused on such direct effects of CDDP. Even though the inflammatory mechanism plays a critical role in the pathogenesis in ischemic acute renal injury,^{17,36} little information has been available regarding the role of this mechanism in renal damage induced by toxic reagents such as CDDP. However, recent reports demonstrated that inflammation is important in CDDP-induced renal damage.⁸⁻¹⁰ Ramesh and Reeves¹⁰ reported that inhibitors of tumor necrosis factor- α ameliorate CDDP-induced renal dysfunction. Therefore, the present study not only supports the importance of inflammation in this model, but also provides an interesting molecular target for prevention of CDDP-induced renal dysfunction.

Because the ODN is preferentially absorbed by the proximal tubule epithelial cells,^{37,38} preventive administration of the MK anti-sense ODN would be a candidate therapy for CDDP-induced renal dysfunction. The present data support the potential of MK as a candidate molecular target for the prevention of CDDP-induced renal dysfunction.

References

1. Kuhlmann MK, Burkhardt G, Köhler H: Insights into potential cellular mechanisms of cisplatin nephrotoxicity and their clinical application. *Nephrol Dial Transplant* 1997, 12:2478-2480
2. Leibbrandt ME, Wolfgang GH, Metz AL, Ozobia AA, Haskins JR: Critical subcellular targets of cisplatin and related platinum analogs in rat renal proximal tubule cells. *Kidney Int* 1995, 48:761-770
3. Rosenberg JM, Sato PH: Cisplatin inhibits *in vitro* translation by pre-

- venting the formation of complete initiation complex. *Mol Pharmacol* 1993, 43:491–497
4. Courjault-Gautier F, Le Grimellec C, Giocondi MC, Toutain HJ: Modulation of sodium-coupled uptake and membrane fluidity by cisplatin in renal proximal tubular cells in primary culture and brush-border membrane vesicles. *Kidney Int* 1995, 47:1048–1056
 5. Bompard G: Cisplatin-induced changes in cytochrome P-450, lipid peroxidation and drug-metabolizing enzyme activities in rat kidney cortex. *Toxicol Lett* 1989, 48:193–199
 6. Mistry P, Merazga Y, Spargo DJ, Riley PA, McBrien DC: The effects of cisplatin on the concentration of protein thiols and glutathione in the rat kidney. *Cancer Chemother Pharmacol* 1991, 28:277–282
 7. Zhang JG, Lindup WE: Role of mitochondria in cisplatin-induced oxidative damage exhibited by rat renal cortical slices. *Biochem Pharmacol* 1993, 45:2215–2222
 8. Kelly KJ, Meehan SM, Colvin RB, Williams WW, Bonventre JV: Protection from toxicant-mediated renal injury in the rat with anti-CD54 antibody. *Kidney Int* 1999, 56:922–931
 9. Deng J, Kohda Y, Chiao H, Wang Y, Hu X, Hewitt SM, Miyaji T, McLeroy P, Nibhanupody B, Li S, Star RA: Interleukin-10 inhibits ischemic and cisplatin-induced acute renal injury. *Kidney Int* 2001, 60:2118–2128
 10. Ramesh G, Reeves WB: TNF-alpha mediates chemokine and cytokine expression and renal injury in cisplatin nephrotoxicity. *J Clin Invest* 2002, 110:835–842
 11. Muramatsu T: Midkine and pleiotrophin: two related proteins involved in development, survival, inflammation and tumorigenesis. *J Biochem (Tokyo)* 2002, 132:359–371
 12. Kurtz A, Schulte AM, Wellstein A: Pleiotrophin and midkine in normal development and tumor biology. *Crit Rev Oncol* 1995, 6:151–177
 13. Vilar J, Lalou C, Duong VH, Charrin S, Hardouin S, Raulais D, Merlet-Bénichou C, Lelièvre-Pégorier M: Midkine is involved in kidney development and in its regulation by retinoids. *J Am Soc Nephrol* 2002, 13:668–676
 14. Kadomatsu K, Tomomura M, Muramatsu T: cDNA cloning and sequencing of a new gene intensely expressed in early differentiation stages of embryonal carcinoma cells and in mid-gestation period of mouse embryogenesis. *Biochem Biophys Res Commun* 1988, 151:1312–1318
 15. Kadomatsu K, Huang RP, Suganuma T, Murata F, Muramatsu T: A retinoic acid responsive gene MK found in the teratocarcinoma system is expressed in spatially and temporally controlled manner during mouse embryogenesis. *J Cell Biol* 1990, 110:607–616
 16. Mitsiadis TA, Muramatsu T, Muramatsu H, Thesleff I: Midkine (MK), a heparin-binding growth/differentiation factor, is regulated by retinoic acid and epithelial-mesenchymal interactions in the developing mouse tooth, and affects cell proliferation and morphogenesis. *J Cell Biol* 1995, 129:267–281
 17. Sato W, Kadomatsu K, Yuzawa Y, Muramatsu H, Hotta N, Matsuo S, Muramatsu T: Midkine is involved in neutrophil infiltration into the tubulointerstitium in ischemic renal injury. *J Immunol* 2001, 167:3463–3469
 18. Qi M, Ikematsu S, Ichihara-Tanaka K, Sakuma S, Muramatsu T, Kadomatsu K: Midkine rescues Wilms' tumor cells from cisplatin-induced apoptosis: regulation of Bcl-2 expression by midkine. *J Biochem (Tokyo)* 2000, 127:269–277
 19. Owada K, Sanjo N, Kobayashi T, Mizusawa H, Muramatsu H, Muramatsu T, Michikawa M: Midkine inhibits caspase-dependent apoptosis via the activation of mitogen-activated protein kinase and phosphatidylinositol 3-kinase in cultured neurons. *J Neurochem* 1999, 73:2084–2092
 20. Takada T, Toriyama K, Muramatsu H, Song XJ, Torii S, Muramatsu T: Midkine, a retinoic acid-inducible heparin-binding cytokine in inflammatory responses: chemotactic activity to neutrophils and association with inflammatory synovitis. *J Biochem (Tokyo)* 1997, 122:453–458
 21. Horiba M, Kadomatsu K, Nakamura E, Muramatsu H, Ikematsu S, Sakuma S, Hayashi K, Yuzawa Y, Matsuo S, Kuzuya M, Kaname T, Hirai M, Saito H, Muramatsu T: Neointima formation in a restenosis model is suppressed in midkine-deficient mice. *J Clin Invest* 2000, 105:489–495
 22. Qi M, Ikematsu S, Maeda N, Ichihara-Tanaka K, Sakuma S, Noda M, Muramatsu T, Kadomatsu K: Haptotactic migration induced by midkine. Involvement of protein-tyrosine phosphatase zeta. Mitogen-activated protein kinase, and phosphatidylinositol 3-kinase. *J Biol Chem* 2001, 276:15868–15875
 23. Unoki K, Ohba N, Arimura H, Muramatsu H, Muramatsu T: Rescue of photoreceptors from the damaging effects of constant light by midkine, a retinoic acid-responsive gene product. *Invest Ophthalmol Vis Sci* 1994, 35:4063–4068
 24. Yoshida Y, Ikematsu S, Moritoyo T, Goto M, Tsutsui J, Sakuma S, Osame M, Muramatsu T: Intraventricular administration of the neurotrophic factor midkine ameliorates hippocampal delayed neuronal death following transient forebrain ischemia in gerbils. *Brain Res* 2001, 894:46–55
 25. Kadomatsu K, Hagihara M, Akhter S, Fan QW, Muramatsu H, Muramatsu T: Midkine induces the transformation of NIH3T3 cells. *Br J Cancer* 1997, 75:354–359
 26. Nakamura E, Kadomatsu K, Yuasa S, Muramatsu H, Mamiya T, Nabeshima T, Fan QW, Ishiguro K, Igakura T, Matsubara S, Kaname T, Horiba M, Saito H, Muramatsu T: Disruption of the midkine gene (Mdk) resulted in altered expression of a calcium binding protein in the hippocampus of infant mice and their abnormal behaviour. *Genes Cells* 1998, 3:811–822
 27. Nomura A, Nishikawa K, Yuzawa Y, Okada H, Okada N, Morgan BP, Piddlesden SJ, Nadai M, Hasegawa T, Matsuo S: Tubulointerstitial injury induced in rats by a monoclonal antibody that inhibits function of a membrane inhibitor of complement. *J Clin Invest* 1995, 96:2348–2356
 28. Wuthrich RP, Glimcher LH, Yui MA, Jevnikar AM, Dumas SE, Kelley VE: MHC class II, antigen presentation and tumor necrosis factor in renal tubular epithelial cells. *Kidney Int* 1990, 37:783–792
 29. Kamijo T, Zindy F, Roussel MF, Quelle DE, Downing JR, Ashmun RA, Grosveld G, Sherr CJ: Tumor suppression at the mouse INK4a locus mediated by the alternative reading frame product p19ARF. *Cell* 1997, 91:649–659
 30. Kadomatsu K, Anzano MA, Slayter MV, Winokur TS, Smith JM, Sporn MB: Expression of sulfated glycoprotein 2 is associated with carcinogenesis induced by N-nitroso-N-methylurea in rat prostate and seminal vesicle. *Cancer Res* 1993, 53:1480–1483
 31. Takei Y, Kadomatsu K, Matsuo S, Itoh H, Nakazawa K, Kubota S, Muramatsu T: Antisense oligodeoxynucleotide targeted to midkine, a heparin-binding growth factor, suppresses tumorigenicity of mouse renal carcinoma cells. *Cancer Res* 2001, 61:8486–8491
 32. Ishikawa T, Ali-Osman F: Glutathione-associated cis-diamminedichloroplatinum(II) metabolism and ATP-dependent efflux from leukemia cells. Molecular characterization of glutathione-platinum complex and its biological significance. *J Biol Chem* 1993, 268:20116–20125
 33. Bernareggi A, Torti L, Facino RM, Carini M, Depta G, Casetta B, Farrell N, Spadacini S, Ceserani R, Tognella S: Characterization of cisplatin-glutathione adducts by liquid chromatography-mass spectrometry. Evidence for their formation in vitro but not in vivo after concomitant administration of cisplatin and glutathione to rats and cancer patients. *J Chromatogr B Biomed Appl* 1995, 669:247–263
 34. Townsend DM, Deng M, Zhang L, Lapus MG, Hanigan MH: Metabolism of cisplatin to a nephrotoxin in proximal tubule cells. *J Am Soc Nephrol* 2003, 14:1–10
 35. Hanigan MH, Lykissa ED, Townsend DM, Ou CN, Barrios R, Lieberman MW: Gamma-glutamyl transpeptidase-deficient mice are resistant to the nephrotoxic effects of cisplatin. *Am J Pathol* 2001, 159:1889–1894
 36. Sheridan AM, Bonventre JV: Cell biology and molecular mechanisms of injury in ischemic acute renal failure. *Curr Opin Nephrol Hypertens* 2000, 9:427–434
 37. Oberbauer R, Schreiner GF, Meyer TW: Renal uptake of an 18-mer phosphorothioate oligonucleotide. *Kidney Int* 1995, 48:1226–1232
 38. Oberbauer R, Schreiner GF, Biber J, Murer H, Meyer TW: In vivo suppression of the renal Na⁺/Pi cotransporter by antisense oligonucleotides. *Proc Natl Acad Sci USA* 1996, 93:4903–4906